Indirect coupling between $Ca_v1.2$ channels and ryanodine receptors to generate Ca^{2+} sparks in murine arterial smooth muscle cells

Kirill Essin[1,2], Andrea Welling[3], Franz Hofmann[3], Friedrich C. Luft[2], Maik Gollasch[1,2] and Sven Moosmang[3]

[1]*Department of Nephrology and Medical Intensive Care, Charité Campus Virchow-Klinikum, Berlin, Germany*
[2]*Franz Volhard Clinic, HELIOS Klinikum Berlin, Charité Campus Berlin-Buch, and Max Delbrück Center for Molecular Medicine, Berlin, Germany*
[3]*Department of Pharmacology and Toxicology, Technical University München, Munich, Germany*

In arterial vascular smooth muscle cells (VSMCs), Ca^{2+} sparks stimulate nearby Ca^{2+}-activated K^+ (BK) channels that hyperpolarize the membrane and close L-type Ca^{2+} channels. We tested the contribution of L-type $Ca_v1.2$ channels to Ca^{2+} spark regulation in tibial and cerebral artery VSMCs using VSMC-specific $Ca_v1.2$ channel gene disruption in (SMAKO) mice and an approach based on Poisson statistical analysis of activation frequency and first latency of elementary events. $Ca_v1.2$ channel gene inactivation reduced Ca^{2+} spark frequency and amplitude by ∼50% and ∼80%, respectively. These effects were associated with lower global cytosolic Ca^{2+} levels and reduced sarcoplasmic reticulum (SR) Ca^{2+} load. Elevating cytosolic Ca^{2+} levels reversed the effects completely. The activation frequency and first latency of elementary events in both wild-type and SMAKO VSMCs weakly reflected the voltage dependency of L-type channels. This study provides evidence that local and tight coupling between the $Ca_v1.2$ channels and ryanodine receptors (RyRs) is not required to initiate Ca^{2+} sparks. Instead, $Ca_v1.2$ channels contribute to global cytosolic $[Ca^{2+}]$, which in turn influences luminal SR calcium and thus Ca^{2+} sparks.

(Resubmitted 19 June 2007; accepted after revision 27 July 2007; first published online 2 August 2007)
Corresponding author M. Gollasch: Charité Campus Virchow Klinikum, Humboldt University, Augustenburger Platz 1, 13353 Berlin, Germany. Email: maik.gollasch@charite.de

Ca^{2+} sparks are optical images of elementary Ca^{2+} release from a single Ca^{2+} release unit (CRU) composed of a group of ryanodine receptors (RyRs) in the sarcoplasmic reticulum (SR) (Wang *et al.* 2004). In arterial vascular smooth muscle cells (VSMCs), membrane depolarizations produce moderate (100–300 nM) increases in the global $[Ca^{2+}]_i$ that produce contraction (Nelson *et al.* 1990). These contractions depend on Ca^{2+} ion influx through $Ca_v1.2$ Ca^{2+} channels (Moosmang *et al.* 2003). Ca^{2+} spark inhibition paradoxically produces vasoconstriction for two reasons (Nelson *et al.* 1995; Knot *et al.* 1998). First, a single spark is capable of producing a very high (10–100 μM) local (∼1% of the cell volume) increase in $[Ca^{2+}]_i$ (Perez *et al.* 1999, 2001) while increasing the global $[Ca^{2+}]_i$ by only < 2 nM (Nelson *et al.* 1995; Jaggar *et al.* 2000). Second, Ca^{2+} sparks occur in close proximity to the cell membrane, where every Ca^{2+} spark activates numerous BK channels (Perez *et al.* 1999; Brenner *et al.* 2000; Pluger *et al.* 2000; Sausbier *et al.* 2005). The resultant 'spontaneous transient outward currents' (STOCs) cause hyperpolarization of the cell membrane, thereby shutting off tonic Ca^{2+} entry through $Ca_v1.2$ channels. Therefore, the net result of the spark–STOC coupling is decreased global $[Ca^{2+}]_i$ and vasorelaxation (Nelson *et al.* 1995; Gollasch *et al.* 1998).

Arterial VSMCs do not exhibit action potentials *in vivo* to elevate global $[Ca^{2+}]_i$. Instead, steady-state membrane VSMC depolarization increases voltage-dependent open probability of L-type channels, global $[Ca^{2+}]_i$, and presumably SR $[Ca^{2+}]$ (Jaggar *et al.* 2000). Ca^{2+} spark frequency at steady-state potentials is modulated by Ca^{2+} influx through L-type Ca^{2+} channels (Nelson *et al.* 1995; Jaggar *et al.* 1998; Remillard *et al.* 2002; Cheng & Jaggar, 2006). However, whether or not local Ca^{2+} influx regulates the probability of these rather 'spontaneous' sparks in arterial VSMCs is unresolved. An elevation in local Ca^{2+} from opening of L-type Ca^{2+} channels, elevated global $[Ca^{2+}]_i$, or increased luminal SR $[Ca^{2+}]$ could each contribute to the observed steady-state depolarization-induced increase in Ca^{2+} spark frequency and amplitude.

This paper has online supplemental material.

DOI: 10.1113/jphysiol.2007.138982

Recently, Santana *et al.* obtained images of brief Ca^{2+} fluxing through single L-type Ca^{2+} channels in arterial VSMCs (Navedo *et al.* 2005). Analogous to cardiomyocytes (Wang *et al.* 2001), these events were named 'Ca^{2+} sparklets'. The authors also detected single or small clusters of L-type channels in VSMCs that operate in a high activity mode, creating sites of nearly continual Ca^{2+} influx ('persistent Ca^{2+} sparklet sites') even at hyperpolarized membrane potentials of 70 mV (Navedo *et al.* 2005, 2006). Sparklets could directly activate RyR to generate Ca^{2+} sparks in VSMCs (Navedo *et al.* 2005). However, a rather loose coupling between Ca^{2+} entry and spark frequency has been deduced from urinary bladder experiments (Collier *et al.* 2000; Kotlikoff, 2003). In contrast to arterial VSMCs, bladder cells typically produce contraction by generating action potentials to induce calcium-induced calcium release through RyRs (Imaizumi *et al.* 1998). However, since arterial smooth muscle produces only small, steady-state membrane depolarizations of a few millivolts to produce sustained calcium influx to elevate global $[Ca^{2+}]_i$, the coupling mechanism between $Ca_v1.2$ and RyRs in arterial smooth muscle is not clear.

Ca^{2+} can activate RyRs on the SR luminal side of the receptor (Ching *et al.* 2000). Recent evidence indicates that the frequency and amplitude of Ca^{2+} sparks depends steeply on the SR Ca^{2+} load in stomach muscle (ZhuGe *et al.* 1999). Experiments using phospholamban-deficient cerebral artery VSMCs supported this notion (Wellman *et al.* 2001). Spark-like Ca^{2+} release has been observed in aortic and cerebral VSMCs after chemical permeabilization of the cell membrane (Rueda & Valdivia, 2006) supporting the idea that spark initiation does not depend on a close L-type Ca^{2+} channel and RyR proximity. We tested the hypothesis that $Ca_v1.2$ channels contribute to global cytosolic calcium, which in turn influences luminal SR calcium and thus Ca^{2+} sparks in arterial VSMCs. We used VSMC-specific $Ca_v1.2$ channel gene inactivation in mice (SMAKO) (Moosmang *et al.* 2003). We provide evidence that rapid, local and tight coupling between the $Ca_v1.2$ channels and RyRs is not required to initiate Ca^{2+} sparks. We found that cytosolic $[Ca^{2+}]_i$ itself contributes minimally to the acute triggering of physiologically relevant proportion of Ca^{2+} sparks. Instead the most eficacious Ca^{2+} spark trigger appears to be the luminal SR Ca^{2+}, which is slowly loaded via Ca^{2+} influx through $Ca_v1.2$ channels.

Methods

All animal experimental protocols were approved by the local animal care committees (Regierung von Oberbayern, Munich, Germany and LaGetSi, Berlin, Germany). The generation of mice deficient in the smooth muscle $Ca_v1.2$ Ca^{2+} channel (SMAKO, smooth muscle α1c-subunit Ca^{2+} channel knockout) has been described (Moosmang *et al.* 2003). Briefly, a conditional *lox*P-flanked allele (L2) of the $Ca_v1.2$ gene (i.e. exons 14 and 15) was generated by homologous recombination in R1 embryonic stem cells. In addition, mice carried a knock-in allele (SM-CreER T2 (ki)) (Kuhbandner *et al.* 2000), which expresses the tamoxifen-dependent Cre recombinase, CreER T2, from the endogenous SM22 α gene locus, which is selectively expressed in smooth muscle of adult mice. Thus, tamoxifen treatment of mice results in conversion of the *lox*P-flanked $Ca_v1.2$ allele (L2) into a Cav1.2 knockout allele (L1) specifically in SMC. Animals were kept under standard conditions with water and food *ad libitum*. At an age of 2–3 months, SMAKO mice ($Ca_v1.2$ l1/L2, SM-CreER T2 (ki)+/.) and corresponding control (CTR) mice ($Ca_v1.2$+/L2, SM-CreER T2 (ki)+/.) were I.P. injected with tamoxifen (2 mg day^{-1}) for five consecutive days. After 3–4 weeks, mice were killed by cervical dislocation and the brain and tibial arteries were removed. Experiments were performed on the same day with arteries from litter-matched control and SMAKO mice.

Isolation of arterial VSMCs

SMCs from tibial and basilar arteries were isolated as described (Gollasch *et al.* 1998; Pluger *et al.* 2000). Briefly, the brain and tibial arteries were removed and quickly transferred to cold (4°C) oxygenated (95% O_2–5% CO_2) physiological salt solution (PSS) of the following composition (mM): 119 NaCl, 4.7 KCl, 25.0 $NaHCO_3$, 1.2 KH_2PO_4, 1.8 $CaCl_2$, 1.2 $MgSO_4$, 0.026 EDTA and 11.1 glucose. The arteries were cleaned, cut into pieces and placed in a Ca^{2+}-free Hanks' solution (mM): 55 NaCl, 80 sodium glutamate, 5.6 KCl, 2 $MgCl_2$, 1 mg ml^{-1} bovine serum albumin (BSA, Sigma), 10 glucose and 10 Hepes (pH 7.4 with NaOH) containing 1.0 mg ml^{-1} papain (Sigma) and 1 mg ml^{-1} DTT for 15 (cerebral arteries) to 45 min (tibial arteries) at 36°C. The segments were then placed in Hanks' solution containing 1 mg ml^{-1} collagenase (Sigma, type F and H; ratio 30% and 70%) and 0.1 mM $CaCl_2$ for 6 min (cerebral arteries) to 10 min (tibial arteries) at 36°C. Following several washes in Ca^{2+}-free Hanks' solution (containing 1 mg ml^{-1} BSA), single cells were dispersed from artery segments by gentle trituration. Cells were then stored in the same solution at 4°C.

Ca^{2+} sparks

VSMCs were seeded onto glass coverslips and incubated with the Ca^{2+} indicator fluo-3-AM (5 μM) and pluronic acid (0.005%; w/v) for 30 min at room temperature in Ca^{2+}-free Hanks' solution (Lohn *et al.* 2000; Pluger *et al.* 2000; Lohn *et al.* 2001*a*). After loading of the cells with fluo-3, the cells were washed with a Hepes-buffered

physiological saline solution (Hepes-PSS) for 30–40 min at room temperature. The Hepes-PSS had the following composition (mM): 135 NaCl, 5.4 KCl, 1.8 $CaCl_2$, 1 $MgCl_2$, 10 Hepes and 10 glucose (pH 7.4 with NaOH). Single SMCs were imaged using a Bio-Rad (Munich, Germany) laser scanning confocal microscope attached to a Nikon Diaphot microscope (Furstenau *et al.* 2000; Lohn *et al.* 2001*a*). Images were obtained by illumination with a krypton–argon laser at 488 nm, and recording all emitted light above 500 nm. Ca^{2+} sparks were measured in Hepes-PSS. Cells were scanned in the 'line scan' mode for 10 s. Ca^{2+} spark analysis was performed off-line using custom software written in C++ by K. Essin. Ca^{2+} sparks were defined as local fractional fluorescence increases greater than 1.2. The site of a Ca^{2+} spark was determined as the centre of the spark at the time of its initiation. Ca^{2+} spark width was determined at 50% maximal amplitude; decay was measured from peak to half-maximal amplitude. The frequency was estimated as the number of detected sparks divided by the total scan time. The amplitudes were expressed as fractional fluorescence increase (F/F_0) or in absolute values relative to the global resting cytosolic $[Ca^{2+}]$ using the following equation: (Cheng *et al.* 1993; Jaggar *et al.* 1998; Herrera *et al.* 2001)

$$\Delta[Ca^{2+}]_{spark} = KR/(K/[Ca^{2+}]_r + 1 - R) - [Ca^{2+}]_r \quad (1)$$

where R is the fractional fluorescence increase (F/F_0), $[Ca^{2+}]_r$ is the free resting cytosolic Ca^{2+} concentration, and K is the apparent affinity of fluo-3 for Ca^{2+} (400 nM) (Cheng *et al.* 1993). $[Ca^{2+}]_r$ was measured directly using Fura-2 in separate experiments (see below).

In the experiments to determine the first latency to occurrence of a Ca^{2+} spark after membrane depolarization, fast two-dimensional confocal microscopy was used in VSMCs clamped by the perforated whole-cell patch technique (see below). Cells were loaded with fluo-4-AM (5 μM) and pluronic acid (0.005%; w/v) for 30 min at room temperature in Ca^{2+}-free solution (mM: 10 Hepes, 55 NaCl, 5.6 KCl, 80 sodium glutamate, 2 $MgCl_2$, and 10 D-glucose; pH to 7.4 with NaOH) and washed for 30 min with Ca^{2+}containing solution (for external solution for STOC recording, see below). Cells were clamped at −40 mV and depolarized according to the protocol presented in the online Supplemental Fig. 2, similar to that in Lopez-Lopez *et al.* (1995). Synchronicity of the command voltage onset and fluorescence measurment was achieved by means of light-emitting diode placed near the recording chamber and switched on and off from a D/A output of CED 1401 interface before and after the acqusition protocol. Images were taken at 25–50 frames s^{-1} on a PerkinElmer, Nipkow disc-based UltraView LCI confocal scanner linked to a fast digital camera. The confocal system was mounted in an inverted Diaphot microscope with a ×40 oil-immersion objective (NA 1.3; Nikon). Fluo-4 was excited by the 488 nm line of an argon ion laser and emitted fluorescence was collected at wavelengths > 515 nm. Image analysis was done using PerkinElmer's ImagingSuite 5.2 software. Average fluorescence intensity outside of the cell was subtracted from the mean fluorescence intensities to correct for background fluorescence. After background correction, fluorescence *versus* time traces were further analysed in Origin 6.1 (OriginLab Corp., Northampton, MA, USA) and represent the averaged fluorescence from a region of interest (ROI) centred on the spark generating area. This ROI size was determined empirically to be the best compromise between temporal and spatial precision of Ca^{2+} sparks and the signal to noise ratio. Ca^{2+} spark amplitude was expressed as relative fluorescence increase F/F_0, where F is the peak fluorescence and F_0 is the baseline fluorescence in the ROI before Ca^{2+} spark appearance. The latency of occurrence of Ca^{2+} sparks was measured as the time elapsed from the onset of the pulse depolarization to the moment when Ca^{2+} spark amplitude reached 5–10% of its maximum.

K^+ current recordings

K^+ currents were measured by the conventional whole-cell or perforated whole-cell patch technique (Gollasch *et al.* 1996; Lohn *et al.* 2001*a*). In perforated patch recordings, whole cell access was achieved by amphotericin B within 10 min of seal formation at room temperature (20–24°C). Amphotericin B (Sigma) was dissolved in dimethyl sulfoxide (DMSO) and diluted into the pipette solution to 200 μg ml^{-1}. Patch pipettes (resistance, 3–5 MΩ) were filled with a solution containing (mM): 110 potassium aspartate, 30 KCl, 10 NaCl, 1 $MgCl_2$, 10 Hepes and 0.05 EGTA (pH 7.2). The external solution contained (mM): 134 NaCl, 6 KCl, 1 $MgCl_2$, 2 $CaCl_2$, 10 glucose and 10 Hepes (pH 7.4).

To clamp the global $[Ca^{2+}]_i$ at different levels, STOCs were recorded in the conventional whole-cell mode using the following pipette solutions (mM): 80 potassium aspartate, 50 KCl, 10 NaCl, 1 $MgCl_2$, 3 MgATP, 10 Hepes, 10 EGTA and different $[CaCl_2]_i$ (pH 7.2). $[CaCl_2]_i$ were 0.01, 4 and 8 mM and equalled 0.18, 120 and 1000 nM free cytosolic $[Ca^{2+}]$. The free cytosolic $[Ca^{2+}]$ was calculated by the 'Cabuf' program written by Prof G. Droogmans (available at ftp.cc.kuleuven.ac.be/pub/droogmans/cabuf.zip) and based on the stability constants given by Fabiato & Fabiato (1979). To set the free $[Ca^{2+}]_i$ at ∼100 nM and the free $[EGTA]_i$ at different levels, STOCs were recorded in the conventional whole-cell mode using the following pipette solutions (mM): (a) 80 potassium aspartate, 45 KCl, 10 NaCl, 1 $MgCl_2$, 3 MgATP, 10 Hepes, 17 EGTA and 7 $CaCl_2$ (pH 7.2 with KOH) – (∼10 mM free $[EGTA]_i$, ∼100 nM free $[Ca^{2+}]_i$); or (b) 80 potassium aspartate, 45 KCl, 10 NaCl, 1 $MgCl_2$, 3 MgATP, 30 glucose,

10 Hepes, 1.7 EGTA and 0.7 $CaCl_2$ (pH 7.2 with KOH) – (~1 mM free $[EGTA]_i$, ~100 nM free $[Ca^{2+}]_i$); or (c) 80 potassium aspartate, 45 KCl, 10 NaCl, 1 $MgCl_2$, 3 MgATP, 30 glucose, 10 Hepes, 0.17 EGTA and 0.07 $CaCl_2$ (pH 7.2 with KOH) – (~0.1 mM free $[EGTA]_i$, ~100 nM free $[Ca^{2+}]_i$). When indicated, 20 μM Fluo4-AM was added into the pipette solutions to monitor caffeine-induced Ca^{2+} release. Whole cell currents were recorded 5–7 min after disruption of the membrane.

Whole cell currents were recorded using an EPC 7 amplifier (List, Darmstadt, Germany), digitized at 5 kHz, using a CED 1401 series interface (Cambridge Electronic Design Ltd, Cambridge, UK), and CED patch and voltage clamp software version 6.08 or an EPC9 amplifier under contol of Pulse software (HEKA Electronik, Lambrecht, Germany). STOC latency to occurrence upon membrane depolarization was measured using the pulse protocol shown in the online Supplemental Fig. 2, similar to that in Lopez-Lopez *et al.* (1995). The latency of occurrence (or waiting time) of STOCs was measured as the time elapsed from the onset of the pulse depolarization to the peak of STOC minus 15 ms (average time to peak). STOC analysis was performed off-line using custom software written in C++ by K. Essin or Origin 6.1.

Recording of global intracellular $[Ca^{2+}]$

Intracellular $[Ca^{2+}]_i$ was monitored at ~35°C as described (Gollasch *et al.* 1991). Briefly, isolated tibial myocytes were loaded with 3 μM Fura-2-AM for 30 min in buffer solution (mM: 137 NaCl, 5.4 KCl, 1.8 $CaCl_2$, 1 $MgCl_2$, 10 Hepes and 5.6 glucose). In some experiments, cells were incubated with EGTA-AM at different concentrations (10 min) after the Fura-2-AM loading. $[Ca^{2+}]_i$ was continuously recorded as fluorescence intensity (at 510 nm) at alternating 350 (F_{350}) and 380 nm (F_{380}) excitation wavelengths and their respective ratio (F_{350}/F_{380}) by using TILL vision devices (www.till-photonics.de). $[Ca^{2+}]$ was calculated using the following equation:

$$[Ca^{2+}] = K_d\beta(R - R_{min})/(R_{max} - R), \qquad (2)$$

with R_{min} and R_{max} measured from ionomycin treated cells, and $K_d\beta$ determined (Moosmang *et al.* 2003). The pooled mean values for R_{max}, R_{min} and $K_d\beta$ were 8.97, 1.68 and 307 nM, respectively. Stimulation was performed by local application of caffeine (10 mM) via a syringe device. The resting global cytosolic $[Ca^{2+}]_r$ was used for estimation of Ca^{2+} spark amplitudes.

Materials

Fluo-3-AM, Fluo-4-AM, EGTA-AM and Fura-2-AM were purchased from Molecular Probes (Eugene, OR, USA). Stock solutions (0.25 mM) of fluo-3-AM were made using DMSO as the solvent. Ryanodine was obtained from Calbiochem (Bad Soden, Germany). All salts and other drugs were obtained from Sigma-Aldrich (Deisenhofen, Germany) or Merck (Darmstadt, Germany). High external potassium solutions were made by iso-osmotic substitution of NaCl with KCl in the PSS.

All values are given as means ± S.E.M. Data were compared with Student's *t* test ($P < 0.05$). The term '*n*' represents the cell number tested.

Results

Elementary SR release in SMAKO cells

Figure 1*A* shows confocal line-scan images of representative tibial artery VSMC isolated from control and SMAKO mice. Ca^{2+} sparks were observed only in close proximity to the cell surface in both control and SMAKO cells. Ca^{2+} sparks in control cells had an estimated mean amplitude of 418 ± 26 nM, a mean rise time of 22.4 ± 1.3 ms, a decay half-life of 51.6 ± 4.4 ms, and a width at half-maximal amplitude of 3.3 ± 0.1 μm. The frequency of Ca^{2+} sparks was 1.1 ± 0.1 Hz ($n = 162$; Fig. 1*B*). In contrast, Ca^{2+} spark frequency and amplitude were reduced by ~50% and ~80% in SMAKO cells, compared to control cells. The Ca^{2+} spark frequency and estimated spark amplitude were 0.6 ± 0.1 Hz and 55 ± 7 nM in SMAKO cells ($n = 79$ cells) (Fig. 1*B*). However, the rise time, decay and width of Ca^{2+} sparks were not different in SMAKO cells. The mean rise time, decay and width were 20.8 ± 1.8 ms, 48.7 ± 5.9 ms and 3.2 ± 0.2 μm, respectively ($n = 40$ cells). Similar effects were observed in cerebral artery VSMCs (online Supplemental Fig. 1). Since SMAKO cells lack functional L-type $Ca_v1.2$ Ca^{2+} channels (Moosmang *et al.* 2003), the data indicate that $Ca_v1.2$ channels play an important role in the generation of VSMC Ca^{2+} sparks.

Simultaneous optical whole cell and electrical measurements indicate that virtually all Ca^{2+} sparks cause STOCs in arterial myocytes (Perez *et al.* 1999). We recorded STOCs to monitor elementary SR Ca^{2+} release events in VSMC from both wild-type and SMAKO mice. At steady-state membrane potentials of −40 mV, STOCs had a frequency of 2.6 ± 0.4 Hz, a mean amplitude of 28 ± 6 pA, a rise time of 14.8 ± 0.9 ms, and a decay time of 26.1 ± 2.5 ms in control cells ($n = 12$ cells) (Fig. 2). This membrane potential is similar to that of VSMC in intact pressurized arteries (Nelson *et al.* 1990). In contrast, the frequency and amplitude of STOCs at −40 mV were reduced by ~50% in SMAKO cells, compared to control cells (Fig. 2). However, we detected no difference in the rise and decay times in SMAKO cells (Fig. 2*B*). In SMAKO cells, STOCs had a frequency of 0.9 ± 0.4 Hz, a mean amplitude of 13 ± 2 pA, a rise time of 12.8 ± 1.3 and a decay time of 19.6 ± 2.4 ($n = 12$ cells) (Fig. 2*B*). At −20 mV and 0 mV, which represent voltages

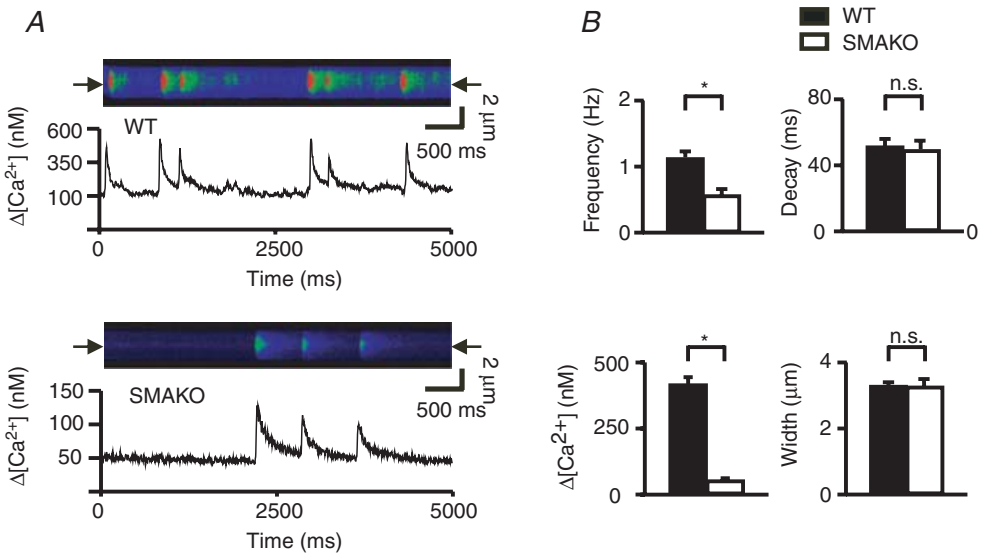

Figure 1. Ca^{2+} sparks in control and SMAKO tibial VSMC
A, upper panel, confocal line-scan image of fluo-3-loaded wild-type (WT) cell with the time course of Ca^{2+} sparks indicated below. The fluorescence time course of the Ca^{2+} sparks was determined over the line indicated by the two arrows. Each line-scan image is a plot of fluorescence along a scanned line (ordinate) *versus* time (abscissa). The line-scan image duration was 5 s, and each line was 4 ms. Lower panel, confocal line-scan image of a fluo-3-loaded SMAKO cell. Amplitudes of Ca^{2+} sparks are expressed as absolute values ($\Delta[Ca^{2+}]_i$) relative to the global resting cytosolic $[Ca^{2+}]_r$ at F_0 using eqn (1). *B*, comparison of spatial–temporal characteristics of Ca^{2+} sparks in WT and SMAKO cells.

at which arterial $Ca_v1.2$ channels exhibit maximal steady-state currents and partial voltage-dependent inactivation, genetic inactivation of $Ca_v1.2$ channels resulted in reduced frequencies and amplitudes of STOCs (Fig. 2*B*). However, the rise and decay times of STOCs were not affected by inactivation of the $Ca_v1.2$ channel gene. Similar effects were observed in cerebral VSMCs (Supplemental Fig. 1). These results suggest that $Ca_v1.2$

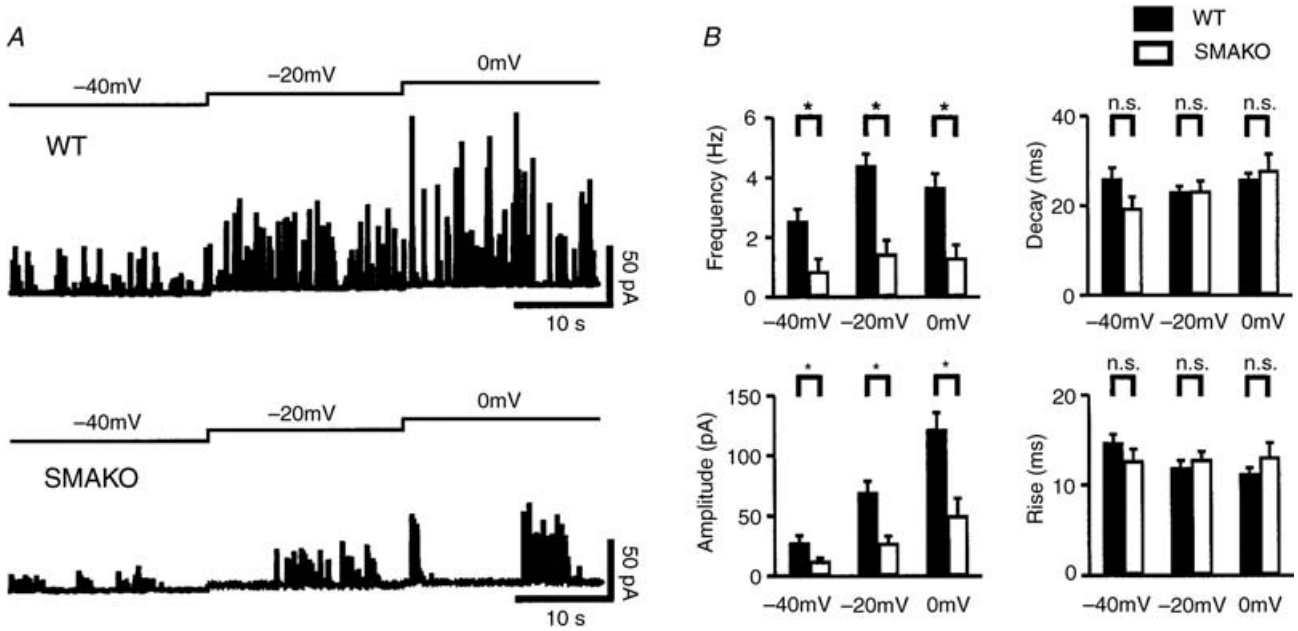

Figure 2. STOCs caused by Ca^{2+} sparks
A, STOCs in representative cells isolated from tibial arteries from control (upper panels, WT) and SMAKO mice (lower panels). The holding potential was stepwise increased in 20 mV increments from −40 mV to 0 mV. *B*, comparison of STOCs characteristics. The holding potential was −40 mV, −20 mV or 0 mV, $*P < 0.05$; n.s., not significant.

channels are involved in the activation of RyR to generate Ca^{2+} sparks. The reduced STOC amplitude in SMAKO cells is consistent with reduced Ca^{2+} spark amplitude, which results in lower subsarcolemmal activator $[Ca^{2+}]$ (< 10–$100\ \mu$M) to activate BK channels.

Effects of dihydropyridines on Ca^{2+}-sparks

Dihydropyridines modulate the open probability of L-type Ca^{2+} channels (Catterall & Striessnig, 1992; Hofmann *et al.* 1999) and therefore should affect spark frequency in wild-type VSMCs. The effects of the dihydropyridines on Ca^{2+} sparks were studied between 1 and 15 min, between 15 and 30 min, and between 30 and 90 min after application of the drugs (Fig. 3*A* and *C*). Nimodipine (1 μM) did not affect Ca^{2+} sparks ($n = 145$), compared to control cells ($n = 115$) in the absence of the drug, when sparks were determined 1–15 min after application of nimodipine. However, nimodipine reduced the Ca^{2+} sparks frequency 15 and 90 min after application (Fig. 3*C*). As expected, the $Ca_v1.2$ channel activator BayK 8644 (1 μM) increased the frequency of Ca^{2+} sparks 60–90 min after application. BayK 8644 and nimodipine did not affect the decay and width of Ca^{2+} sparks (not shown).

A characteristic of the dihydropyridine block is its voltage dependence (Catterall & Striessnig, 1992; Hofmann *et al.* 1999). Consistent with this characteristic, nimodipine (1 μM, 30–90 min) reduced the frequency of Ca^{2+} sparks in control cells depolarized by 30 mM KCl (Fig. 3*A*). In contrast, BayK 8644 (1 μM, 30–90 min), nimodipine (1 μM, 30–90 min) and 30 mM KCl had no effect on the Ca^{2+} spark frequency in SMAKO cells (Fig. 3*B*). Furthermore, nimodipine (1 μM) did not affect the Ca^{2+} spark frequency in SMAKO cells incubated in 30 mM KCl-containing bath solution (Fig. 3*B*). These data are consistent with the above results that functional L-type $Ca_v1.2$ channels modulate Ca^{2+} sparks.

We next measured STOCs in the absence and presence of dihydropyridines and Cd^{2+}. The effects were analysed between 1 and 15 min after drug application. Figure 4 shows that BayK 8644 (1 μM), nimodipine (1 μM) or nimodipine (1 μM) plus the inorganic L-type $Ca_v1.2$ channel blocker Cd^{2+} (100 μM) did not affect STOCs in both control cells and SMAKO tibial artery VSMCs. Similar results were observed in cerebral VSMCs (not shown). However, STOCs were inhibited in control cells by ~50% after 30–90 min application of 1 μM nimodipine (not shown).

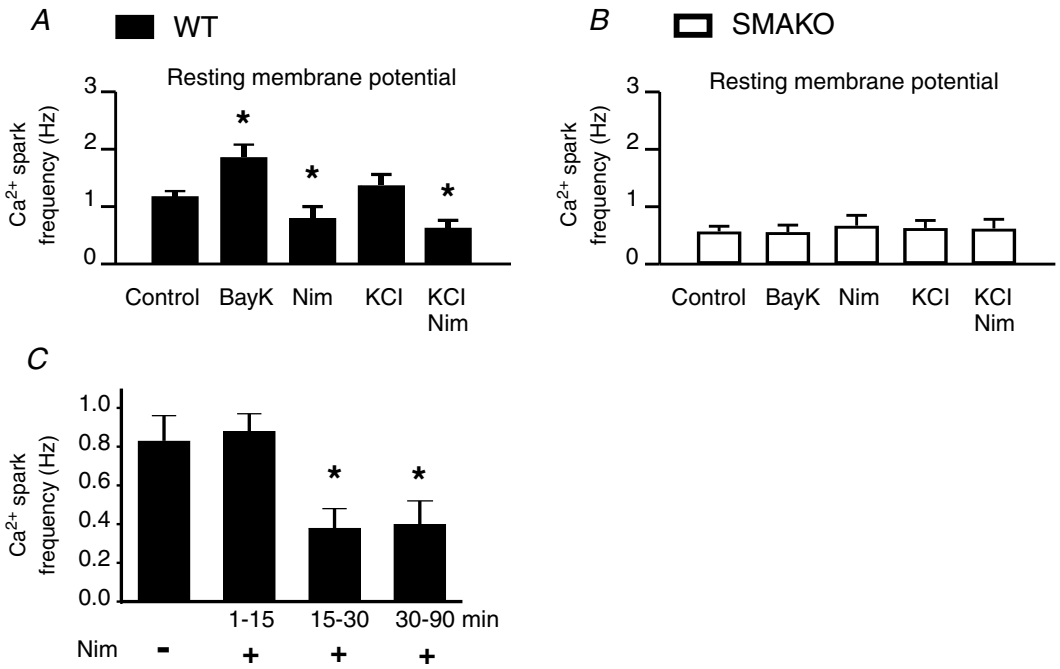

Figure 3. Effects of L-type Ca^{2+} channel modulators on Ca^{2+} spark frequency in control (WT, *A*) and SMAKO (*B*) cells isolated from tibial arteries

Ca^{2+} sparks were recorded in the absence (Control) and presence of 1 μM BayK 8644 (BayK), 1 μM nimodipine (Nim), 30 mM KCl (KCl), and 30 mM KCl plus 1 μM nimodipine (KCl Nim); $n \geq 40$ cells for each group. Cells were preincubated with the compounds for 30–90 min. *C*, summary of Ca^{2+} spark frequency. WT cells from tibial arteries were preincubated with 1 μM nimodipine for 1–15 min, 15–30 min and 30–90 min before the recording. $n \geq 40$ for each group, $^*P < 0.05$.

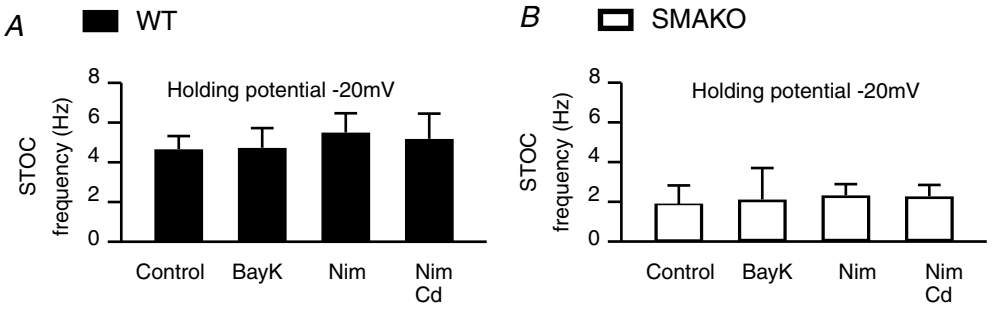

Figure 4. Effects of L-type Ca^{2+} channel modulators on STOC frequencies in wild type (*A*) and SMAKO (*B*) SMCs

Cells were preincubated for 1–15 min with the indicated compounds. STOCs were recorded at a holding potential of −20 mV. STOCs were recorded in the absence (Control) and presence of 1 μM BayK 8644 (BayK), 1 μM nimodipine (Nim), and 1 μM nimodipine plus 300 μM Cd^{2+} (Nim Cd). $n \geq 7$ cells for each group.

The above results clearly indicate that the effects of nimodipine were time dependent but resembled the results obtained with the SMAKO VSMCs (Fig. 3*C*). A simple interpretation of the time dependency might be that the reduced Ca^{2+} spark frequency at the 30–90 min time point was possibly caused by a reduced global $[Ca^{2+}]_i$ and subsequent SR Ca^{2+} load, since the dihydropyridines blocked the major Ca^{2+} influx pathway. This interpretation is in line with the finding that STOCs were not affected by nimodipine at early time points. From these results, we hypothesized further that rather than sensing the local elevation of $[Ca^{2+}]_i$ in the microdomain near the pore of the $Ca_v1.2$ channel, smooth muscle RyRs were not sensitive to the opening of individual $Ca_v1.2$ channels, but rather required a global rise in $[Ca^{2+}]_i$. To test this hypothesis, we first sought to determine whether or not Ca^{2+} influx is required for initiation of Ca^{2+} sparks. Figure 5 shows that removal of external Ca^{2+} reduced the frequency of Ca^{2+} sparks by ∼50% after 15 min in Ca^{2+}-free solution, similar to the effects of Cd^{2+} and nimodipine (Bonev *et al.* 1997). In contrast, after 1–2 min in Ca^{2+}-free solution the spark frequency was not changed (not shown). As a further test, we lowered the global cytosolic $[Ca^{2+}]_i$ using 2-aminoethoxydiphenyl borate (2-APB), which inhibits Ca^{2+} release into the cytosol *via* IP_3 receptors (Peppiatt *et al.* 2003; White & McGeown, 2003; Zima & Blatter, 2004), and blocks store-operated Ca^{2+} influx (Iwasaki *et al.* 2001; Peppiatt *et al.* 2003) through non-selective, Ca^{2+} permeable, cation TRPC channels (van Rossum *et al.* 2000; Clapham *et al.* 2001; Iwasaki *et al.* 2001) and SERCA (Bilmen *et al.* 2002). Figure 5 shows that 2-APB inhibited Ca^{2+} sparks and STOCs, with almost 100% inhibition at 50–100 μM. The effects of 2-APB were observed in the presence and absence of external Ca^{2+}. These observations show that initiation of Ca^{2+} spark release can be regulated by changes of the global $[Ca^{2+}]_i$ and the filling state of SR Ca^{2+} stores independent of the source of Ca^{2+} (influx or release).

RyR stores are exposed to lower global cytosolic $[Ca^{2+}]_i$ in SMAKO cells

Resting $[Ca^{2+}]_i$ was lower in SMAKO cells compared to control cells (∼30 nM *versus* ∼130 nM in SMAKO *versus* control cells) (Fig. 6*B*), suggesting that steady-state

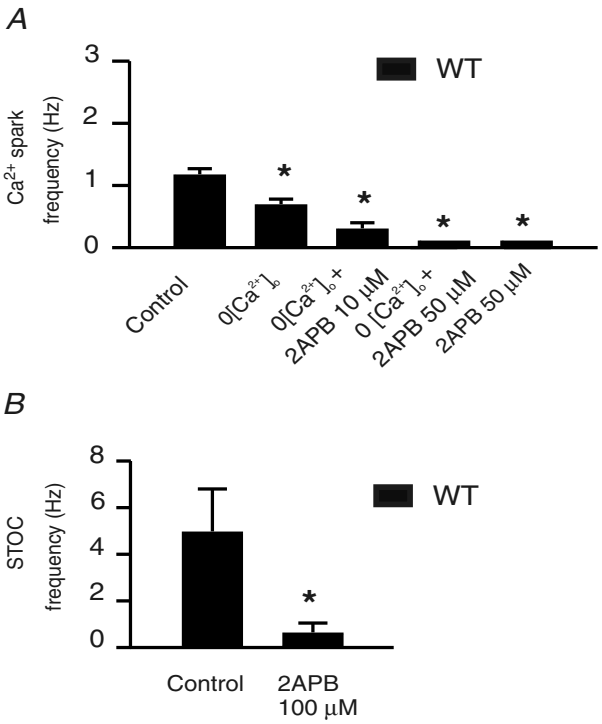

Figure 5. Effects of external Ca^{2+} and 2-aminoethoxydiphenyl borate (2-APB) on Ca^{2+} spark and STOC frequency of control (WT) cells isolated from tibial arteries

A, Ca^{2+} sparks were recorded in the presence of 1.8 mM external Ca^{2+} (Control) and in nominally Ca^{2+}-free solution (0 $[Ca^{2+}]_o$), 0 mM external Ca^{2+} plus 10 μM 2-APB, 0 mM external Ca^{2+} plus 50 μM 2-APB, and 50 μM 2-APB; $n \geq 30$ cells per group. *B*, STOCs were recorded the absence (Control) and presence of 100 μM 2-APB at a holding potential of −20 mV ($n = 5$, each). $^*P < 0.05$.

$[Ca^{2+}]_i$ is tightly controlled by Ca^{2+} influx through $Ca_v1.2$ channels. SR Ca^{2+} load can be analysed by the use of caffeine, which activates each of the RyRs. Caffeine (10 mM) evoked smaller Ca^{2+} transients in SMAKO cells, as compared to control cells (Fig. 6*A* and *C*), indicating that ryanodine-sensitive stores are depleted in SMAKO cells. We used a multipulse application protocol to further characterize the disrupted Ca^{2+} uptake into ryanodine-sensitive stores in SMAKO mice. Eight minutes after a conditioning caffeine pulse, subsequent applications of caffeine (10 mM) induced $[Ca^{2+}]_i$ transients only in control cells, but not in SMAKO VSMCs. Caffeine did not induce $[Ca^{2+}]_i$ elevations at earlier time points in both cell types. The poor recovery of the Ca^{2+} transient in SMAKO VSMCs again suggested that refilling of ryanodine-sensitive Ca^{2+} stores mainly depends on Ca^{2+} influx through $Ca_v1.2$ channels. The results support the interpretation that RyR stores are exposed to lower global cytosolic $[Ca^{2+}]_i$ in SMAKO VSMCs resulting in a reduced driving force for SR Ca^{2+} loading and a reduced SR Ca^{2+} content. Furthermore, the data indicate that $Ca_v1.2$ channels significantly contribute to Ca^{2+} store refilling after Ca^{2+} store depletion in VSMC.

The source leading to increased $[Ca^{2+}]_i$ and SR load is irrelevant for the induction of Ca^{2+} sparks

We next investigated whether or not RyRs are able to sense local Ca^{2+} entry by performing experiments in which we clamped the global $[Ca^{2+}]_i$ at 0.18 nM, 120 nM and 1000 nM while maintaining high mobile intracellular Ca^{2+} buffer (10 mM EGTA). Figure 7*A* shows that STOCs were strongly controlled by the global cytosolic $[Ca^{2+}]_i$ with significantly higher frequencies of STOCs at increasing global $[Ca^{2+}]_i$. Moreover, STOC frequencies were similar in SMAKO and control cells at identical $[Ca^{2+}]_i$ suggesting that the source leading to increased $[Ca^{2+}]_i$ is irrelevant for the induction of Ca^{2+} sparks.

The intimate association between the trigger $Ca_v1.2$ L-type channel and target RyR is not a prerequisite to generate Ca^{2+} sparks. The effective distance between a single L-type $Ca_v1.2$ channel and RyR within the T-tubular membrane in cardiomyocytes has been estimated to be < 100 nm based on the finding that excess concentrations of intracellular mobile slow, high affinity Ca^{2+} buffers such as EGTA (10 mM) do not disrupt the release of Ca^{2+} sparks by L-type Ca^{2+} channel opening (Collier *et al.* 2000). To examine the spatial separation of $Ca_v1.2$ channels and RyRs in VSMCs, we sought to determine whether or not Ca^{2+} sparks disappear in the presence of high concentrations of the membrane-permeant EGTA-AM. As shown in Fig. 7*B*, Ca^{2+} sparks were completely inhibited by 3 mM EGTA-AM (EC_{50} 1 mM), whereas Ca^{2+} sparks were *not* affected in rat cardiomyocytes under similar conditions (EGTA, up to 17 mM) (Collier *et al.* 2000). Caffeine-induced Ca^{2+} release was also inhibited by EGTA-AM in a similar concentration range (Fig. 7*C*), which indicates that the

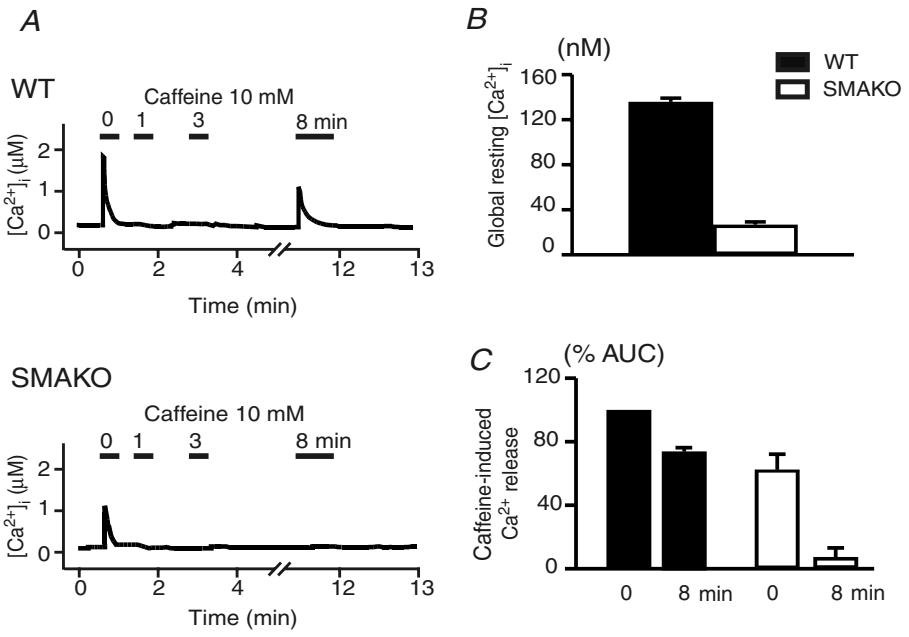

Figure 6. Effects of caffeine on $[Ca^{2+}]_i$ in control (WT) and SMAKO cells isolated from tibial arteries
A, time course of caffeine's effect on $[Ca^{2+}]_i$. Horizontal lines indicate the presence of caffeine (10 mM) in the bath solution. *B*, comparison of resting $[Ca^{2+}]_i$ in WT and SMAKO cells ($n = 70$, each). *C*, comparison of 10 mM caffeine-induced Ca^{2+} release in WT and SMAKO cells ($n = 74$ cells for each group). $[Ca^{2+}]_i$ increases induced by the first application of caffeine (0 min) and after a time interval of 8 min are compared. The Ca^{2+} responses are normalized to the effects (100% response) of 10 mM caffeine in WT cells at 0 min. AUC, areas under the curve.

effects of EGTA-AM may result from reduced global $[Ca^{2+}]_i$ and/or reduced SR Ca^{2+} content. To differentiate between these possibilities, we performed whole-cell recordings of STOCs and clamped the free cytosolic $[Ca^{2+}]$ at ~100 nM and the free $[EGTA]_i$ at 0.1, 1 and 10 mM (see methods for solution compositions). Figure 8*A* shows that despite similar free $[Ca^{2+}]_i$ the frequency and amplitude of STOCs decreased with increasing concentrations of free $[EGTA]_i$. Free $[EGTA]_i$ at 10 mM almost completely abolished STOCs at −40 mV. Figure 8*B* shows that these changes were associated with a reduced SR Ca^{2+} content, as indicated from reduced caffeine-induced Ca^{2+} release. Thus, in contrast to cardiomyocytes, $[EGTA]_i$ at 10 mM inhibits the generation of VSMC Ca^{2+} sparks by depletion of ryanodine-sensitive SR Ca^{2+} stores.

Triggering of Ca^{2+} sparks is not controlled by rapid, direct cross-talk between $Ca_v1.2$ channels and RyRs. We next studied cross-signalling between L-type channels and RyRs using an approach based on Poisson statistical analysis of frequency of activation and first latency of elementary events (Lopez-Lopez *et al.* 1995; Klein *et al.* 1997; Cleemann *et al.* 1998; Collier *et al.* 1999). To satisfy the assumption underlying the Poisson distribution that open events are rare, we monitored elementary Ca^{2+} release events in cells treated with an L-type channel blocker upon depolarization steps (Supplemental Fig. 2). Elementary Ca^{2+} release events were first recorded by direct confocal imaging of Ca^{2+} sparks in wild-type cells treated with 300 nM nimodipine. Figure 9*A* represents histograms of the latencies from the beginning of the depolarization to the time of occurrence of the first identified sparks – first-latency histograms. The amplitude of Ca^{2+} sparks was independent of voltage (Fig. 9*B*), which is similar to cardiac and skeletal muscle (Lopez-Lopez *et al.* 1995; Klein *et al.* 1997; Cleemann *et al.* 1998; Collier *et al.* 1999). However, unlike cardiac and skeletal muscle, the first-latency histograms only slightly depended on the depolarization level and peaked at a relatively positive potential, i.e. ~ +20 mV (Fig. 9*D*) (Lopez-Lopez *et al.* 1995; Klein *et al.* 1997; Cleemann *et al.* 1998; Collier *et al.* 1999). Furthermore, average latencies between −30 mV and +50 mV occurred at ≥ 100 ms (Fig. 9*C*), which is not characteristic for L-type channels (Marks & Jones, 1992; Slesinger & Lansman, 1996) and Ca^{2+} sparks in cardiomyocytes (Lopez-Lopez *et al.* 1995; Klein *et al.* 1997; Cleemann *et al.* 1998; Collier *et al.*

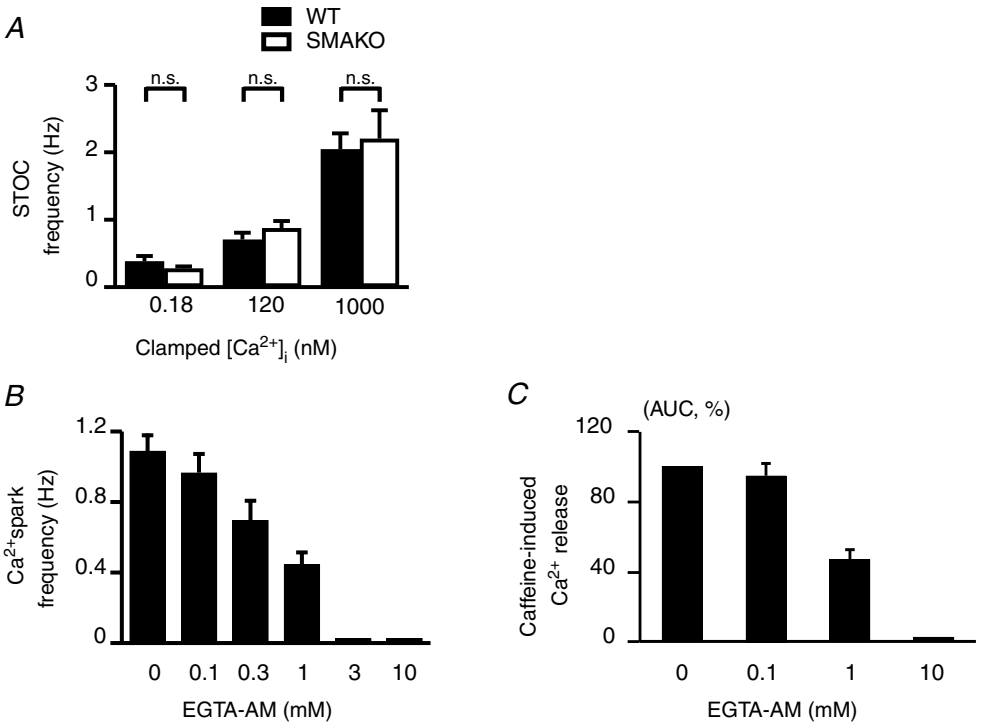

Figure 7. Effects of clamped $[Ca^{2+}]_i$ and EGTA-AM on Ca^{2+} spark, STOC frequency and caffeine-induced Ca^{2+} release in tibial VSMCs

A, STOCs were recorded in the whole-cell mode at −40 mV for 2 min. $[Ca^{2+}]_i$ was clamped to 0.18, 120 or 1000 nM in control (WT) and SMAKO cells ($n \geq 8$, each). *B*, effects of different concentrations of EGTA-AM on Ca^{2+} spark frequency in WT cells ($n \geq 30$, each). *C*, effects of different concentrations of EGTA-AM on caffeine-induced Ca^{2+} release in WT cells ($n \geq 10$, each). The Ca^{2+} responses were normalized to the effect of 10 mM caffeine (100% response) in control cells. AUC, area under the curve.

1999). Thus, the results did not reflect the expected voltage dependency and kinetics of single L-type channels (Lopez-Lopez *et al.* 1995; Cleemann *et al.* 1998; Collier *et al.* 1999). The results were confirmed by electrical STOCs recordings and analysis of first-latency and all-latency histograms (see Results in online Supplemental material, and Supplemental Figs 4–7). The observation that the first-latency and all-latency histograms have different waveforms implies that the release waveform is not determined by the time course of first event activation, with relatively fewer re-openings, as is the case in skeletal and cardiac muscle (Lopez-Lopez *et al.* 1995; Klein *et al.* 1997; Cleemann *et al.* 1998; Collier *et al.* 1999; Shen *et al.* 2004).

Discussion

In cardiac and skeletal muscle, the intimate association between the trigger $Ca_v1.x$ L-type channel and target RyR is a prerequisite to generate Ca^{2+} sparks from single CRU (Cheng *et al.* 1993; Cannell *et al.* 1995; Lopez-Lopez *et al.* 1995; Tsugorka *et al.* 1995; Klein *et al.* 1997; Wang *et al.* 2001). We studied the mechanism and contribution of $Ca_v1.2$ channels in Ca^{2+} spark generation in VSMC by inactivating the VSMC pore-forming $\alpha1$ subunit of the $Ca_v1.2$ channel. Although the importance of the $Ca_v1.2$ Ca^{2+} channel for proper function of arterial VSMCs is beyond reasonable doubt, this study clearly demonstrates that the intimate association between the trigger $Ca_v1.2$ L-type channel and target RyR is a not a prerequisite for the generation of Ca^{2+} sparks in VSMCs.

Rapid, local and tight coupling between the $Ca_v1.2$ channels and RyR is not required

Our data show that $Ca_v1.2$ channels do not directly control RyRs in the CRU *via* elevation of Ca^{2+} locally restricted

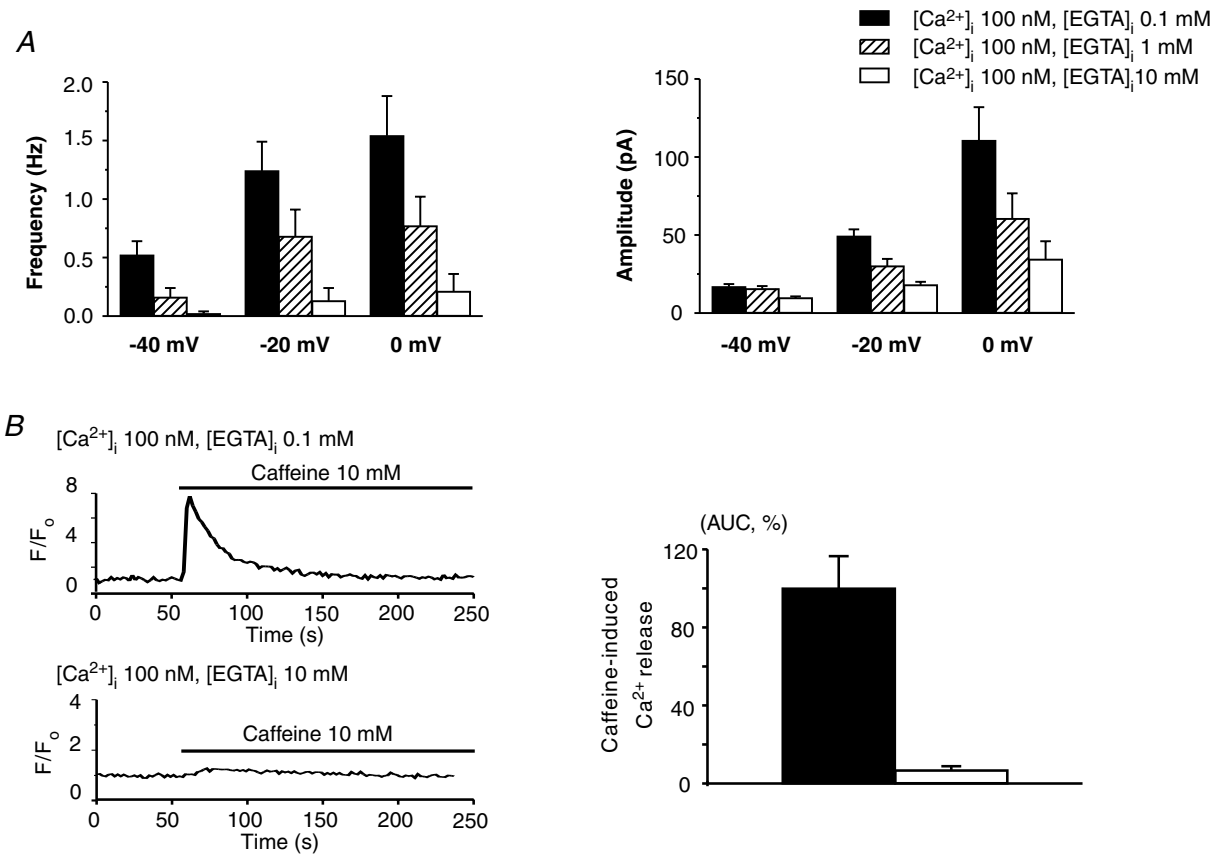

Figure 8. Effects of different $[EGTA]_i$ on STOC frequency and caffeine-induced Ca^{2+} release in tibial VSMCs

The free intracellular Ca^{2+} concentration [Ca] was clamped at 100 nM. *A*, STOC frequency and amplitude recorded in the whole-cell mode at −40, −20 and 0 mV for 2 min. Free $[EGTA]_i$ was set to 0.1, 1 or 10 mM (*n* cells ≥ 10, each concentration); free [Ca] was 100 nM. *B*, left, caffeine-induced Ca^{2+} release in cells loaded with free $[Ca^{2+}]_i$ at 100 nM and free EGTA at 0.1 mM (upper panel) and with free $[Ca^{2+}]_i$ at 100 nM and free EGTA at 10 mM (lower panel). The holding potential was −40 mV. Right, summary of the results. The Ca^{2+} responses were normalized to the effect of 10 mM caffeine (100% response). AUC, areas under the curve. (*n* ≥ 6 cells, each.)

at the cytosolic site of the $Ca_v1.2$ channels in VSMCs. We reach this conclusion for several reasons. First, the effects of nimodipine resembled the results obtained with the SMAKO VSMCs but developed extremely slowly over many minutes. This observation is in contrast to the rapid inhibitory effects of this drug on L-type channels, which can be observed within seconds (Ruth *et al.* 1985; McCarthy & Cohen, 1989; Lohn *et al.* 2002). The failure of nimodipine to induce rapid (within seconds) inhibition of Ca^{2+} sparks indicates that many of the RyRs in the CRU are not directly controlled by high local $[Ca^{2+}]_i$ caused by the opening of adjacent $Ca_v1.2$ channels. Second, the robustness and latency analysis showed that the Ca^{2+} release events did not reflect the voltage dependency and kinetic properties of single L-type channels. In these experiments, we first analysed the histograms of these events using VSMC cells treated with an L-type channel blocker to satisfy Poisson distribution of $Ca_v1.2$ channel openings (Lopez-Lopez *et al.* 1995; Collier *et al.* 1999). Unlike in cardiac muscle, the histograms of these events did not show steep bell-shaped curves characteristic for Ca^{2+} sparks triggered by an elevation in local cytosolic Ca^{2+} from single L-type Ca^{2+} channels (Lopez-Lopez *et al.* 1995; Cleemann *et al.* 1998; Collier *et al.* 1999). In addition, we also found that important features of the nimodipine-treated VSMC histograms, namely those cells with low $Ca_v1.2$ channel activity, did not differ from histograms of control cells (with high $Ca_v1.2$ channel activity) and from SMAKO cells (without $Ca_v1.2$ channels). Third, Ca^{2+} sparks were completely suppressed by excessive concentrations of a slow, high affinity cytosolic Ca^{2+} buffer (millimolar concentrations of EGTA), which suppresses global cytosolic $[Ca^{2+}]$ and causes a slow depletion of ryanodine-sensitive SR Ca^{2+} content in VSMCs, but which should not affect Ca^{2+} communication between $Ca_v1.2$ channels and RyR occurring on the nanometer scale (Stern, 1992; Collier *et al.* 2000). Finally, the substantially reduced frequency

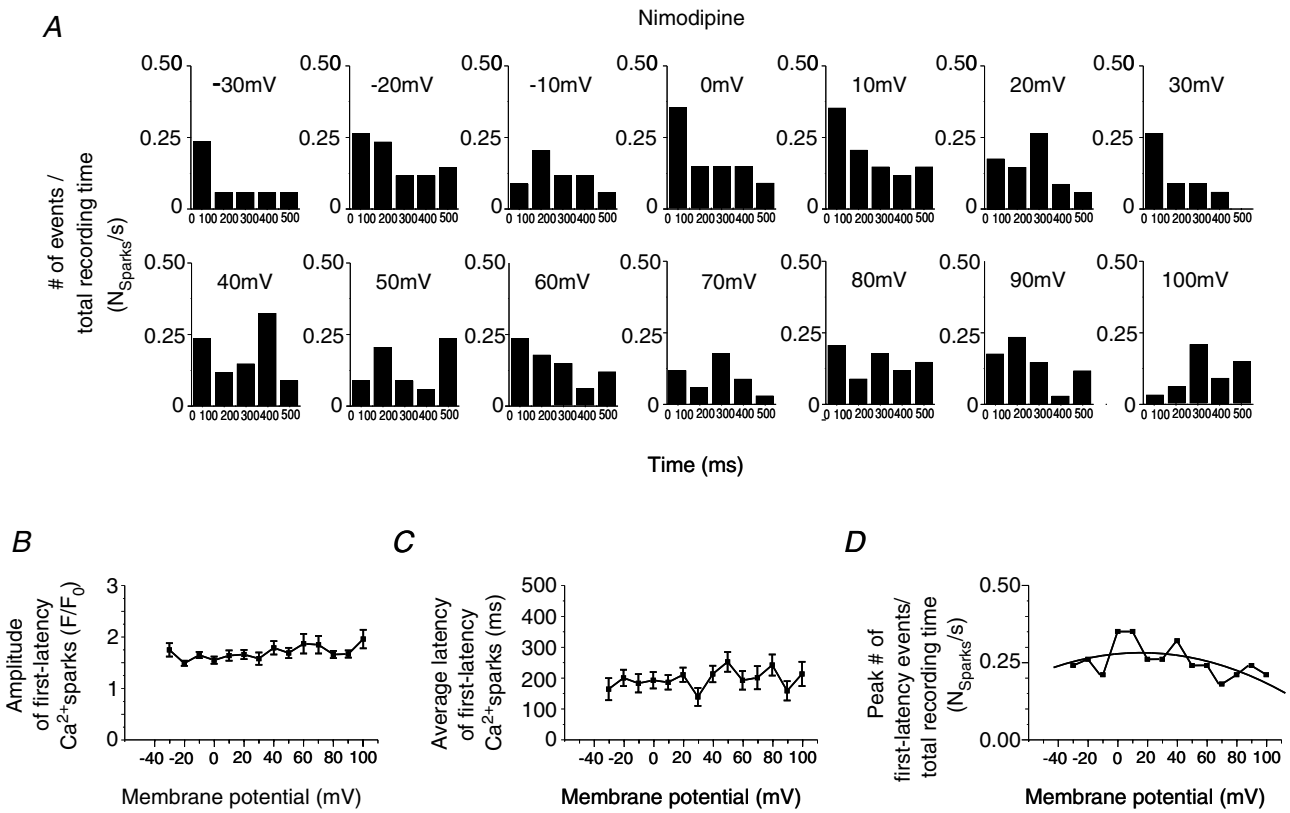

Figure 9. Analysis of first-latency events (Ca^{2+} sparks)
A, histograms of first-latency events from the start of the depolarization to the first identified Ca^{2+} spark. Plots show histograms of latencies to the onset of Ca^{2+} sparks elicited by 500 ms depolarizing pulses to the indicated membrane potentials (−30 mV, −20 mV, −10 mV, 0 mV, +10 mV, +20 mV, +30 mV, +40 mV, +50 mV, +60 mV, +70 mV, +80 mV, +90 mV and +100 mV) for wild-type tibial VSMCs (300 nM nimodipine; $n = 15$ cells of 5 mice). *B*, amplitude of first-latency Ca^{2+} sparks was plotted as a function of the depolarizing voltage. *C*, average latency of first-latency Ca^{2+} sparks was plotted as a function of the depolarizing voltage. *D*, first-latency histogram peak N_{Sparks}/s was plotted as a function of depolarizing voltage. The continuous lines represent polynomial second order fits to the data. Curve fitting revealed maximal values of peak N_{Sparks}/s at 18.8 mV.

and amplitude of Ca^{2+} sparks in SMAKO VSMCs were completely reversed by elevating cytosolic Ca^{2+} levels demonstrating that the source leading to increased global $[Ca^{2+}]_i$ is irrelevant for the induction of Ca^{2+} sparks. Taken together, these results strongly suggest that the intimate association between the trigger $Ca_v1.2$ L-type channel and target RyRs is not crucial for RyRs to generate Ca^{2+} sparks in VSMCs. Therefore, we suggest that the intermolecular mechanisms leading to elementary SR Ca^{2+} release differ substantially between arterial, cardiac and skeletal muscle (Lopez-Lopez *et al.* 1995; Klein *et al.* 1997; Grabner *et al.* 1999; Collier *et al.* 2000; Papadopoulos *et al.* 2004).

$Ca_v1.2$ channels contribute to global cytosolic $[Ca^{2+}]$, which in turn influences luminal SR calcium and thus Ca^{2+} sparks. Our study shows that the substantially reduced frequency and amplitude of Ca^{2+} sparks in SMAKO VSMCs is associated with lower global $[Ca^{2+}]_i$ levels and reduced SR Ca^{2+} load. The data indicate that the cytosolic $[Ca^{2+}]$ is mainly determined by Ca^{2+} influx through $Ca_v1.2$ channels. We provided direct evidence and observed that these effects are completely reversed by elevating cytosolic Ca^{2+} levels (Fig. 7*A*). Our results indicate that cytosolic $[Ca^{2+}]_i$ itself contributes minimally to the acute triggering of the physiologically relevant proportion of Ca^{2+} sparks. This conclusion is based on the following findings. First, RyRs *in situ* are relatively insensitive to global cytosolic Ca^{2+} levels (Jaggar *et al.* 2000). Second, the probability and latency histograms between SMAKO, nimodipine-treated and control cells were not different, despite the fact that the voltage steps used in these experiments induced relatively rapid increases in global $[Ca^{2+}]_i$ from ~100 nM to ~300 nM (within 500 ms to 1 s) in wild-type VSMCs, but not in VSMCs without functional L-type channels (Kamishima & McCarron, 1996; Kamishima *et al.* 2000; Lohn *et al.* 2001*b*). Similar data were obtained in wild-type tibial VSMCs, but not in SMAKO cells (K. Essin & M. Gollasch, unpublished observations). In agreement with these suggestions, rapid (for instance, caffeine or thapsigargin) or slow (phospholamban deficiency) modulation of SR Ca^{2+} load has profound direct effects on both amplitudes and frequency of Ca^{2+} sparks and STOCs, which follows the time course of depletion or uploading SR $[Ca^{2+}]$ (Nelson *et al.* 1995; Bychkov *et al.* 1997; Lohn *et al.* 2001*a*; Wellman *et al.* 2001). Furthermore, increasing levels of cytosolic [EGTA] dramatically reduced both the frequency and amplitude of STOCs in VSMCs, despite $[Ca^{2+}]_i$ being clamped at similar levels, i.e. 100 nM (Fig. 8*A*). These effects were associated with SR Ca^{2+} depletion (Fig. 8*B*) and resembled the effects observed in SMAKO cells. The data indicate that, in VSMCs, the luminal SR Ca^{2+} represents a very important physiological Ca^{2+} signal for activating elementary Ca^{2+} release. The luminal SR Ca^{2+} is controlled by relatively slow Ca^{2+} uptake from the global cytosolic $[Ca^{2+}]$. The advantage of the rigorous SR Ca^{2+} defined regulation of Ca^{2+} sparks is uncoupling spark formation from rapid changes in global cytosolic $[Ca^{2+}]$ to enable a robust and stabile function of the Ca^{2+} spark/STOC pathway to lower global $[Ca^{2+}]$ and vascular tone.

Steady-state Ca^{2+}-influx in SMAKO cells

In SMAKO cells, the global cytosolic $[Ca^{2+}]$ is only 16% of wild-type cells. In contrast, SR Ca^{2+} stores (Fig. 6) and Ca^{2+} spark frequency are reduced by only ~50% in SMAKO cells, which is similar to the effects of nimodipine in wild-type cells. Importantly, the acute removal of Ca^{2+} from the extracellular solution produced effects similar to nimodipine, namely a reduction in the Ca^{2+} spark frequency by ~50%. The remaining Ca^{2+} sparks were completely blocked by 2-APB (Fig. 6). The blocking effects of the IP_3 receptor antagonist 2-APB on Ca^{2+} sparks have been previously reported in portal vein VSMCs. Crosstalk between IP_3 receptors and RyRs has been proposed (Gordienko & Bolton, 2002). Taking into consideration the ability of 2-APB to non-selectively inhibit cation channels, for example TRP related channels (Albert & Large, 2006; Owsianik *et al.* 2006), an alternative explanation could be that ion influx though non-selective cation channels may serve as additional important regulators of Ca^{2+} sparks in arterial VSMCs. Possibly, these channels can function as caveolemmal Ca^{2+} channels that may produce a subpopulation of Ca^{2+} sparks in caveolar microdomains (Lohn *et al.* 2000). Future studies would clarify the possible role of TRP channels in the regulation of Ca^{2+} sparks in VSMCs.

In conclusion, $Ca_v1.2$ channels are important regulatory proteins in the indirect control of Ca^{2+} sparks in arterial VSMCs. We found that $Ca_v1.2$ channel genetic inactivation substantially lowers resting global $[Ca^{2+}]_i$, which in turn reduces slowly luminal SR calcium and thus Ca^{2+} sparks. We found that rapid, local and tight coupling between the $Ca_v1.2$ channels and RyRs is not required to initiate Ca^{2+} sparks. The slow, indirect coupling between $Ca_v1.2$ channels and RyRs is in excellent agreement with the physiological function of Ca^{2+} sparks to serve as robust and stable negative feedback regulators for the global $[Ca^{2+}]_i$ and arterial tone.

References

Albert AP & Large WA (2006). Signal transduction pathways and gating mechanisms of native TRP-like cation channels in vascular myocytes. *J Physiol* **570**, 45–51.

Bilmen JG, Wootton LL, Godfrey RE, Smart OS & Michelangeli F (2002). Inhibition of SERCA Ca^{2+} pumps by 2-aminoethoxydiphenyl borate (2-APB). 2-APB reduces both Ca^{2+} binding and phosphoryl transfer from ATP, by interfering with the pathway leading to the Ca^{2+}-binding sites. *Eur J Biochem* **269**, 3678–3687.

Bonev AD, Jaggar JH, Rubart M & Nelson MT (1997). Activators of protein kinase C decrease Ca^{2+} spark frequency in smooth muscle cells from cerebral arteries. *Am J Physiol Cell Physiol* **273**, C2090–C2095.

Brenner R, Perez GJ, Bonev AD, Eckman DM, Kosek JC, Wiler SW, Patterson AJ, Nelson MT & Aldrich RW (2000). Vasoregulation by the $\beta 1$ subunit of the calcium-activated potassium channel. *Nature* **407**, 870–876.

Bychkov R, Gollasch M, Ried C, Luft FC & Haller H (1997). Regulation of spontaneous transient outward potassium currents in human coronary arteries. *Circulation* **95**, 503–510.

Cannell MB, Cheng H & Lederer WJ (1995). The control of calcium release in heart muscle. *Science* **268**, 1045–1049.

Catterall WA & Striessnig J (1992). Receptor sites for Ca^{2+} channel antagonists. *Trends Pharmacol Sci* **13**, 256–262.

Cheng X & Jaggar JH (2006). Genetic ablation of caveolin-1 modifies Ca^{2+} spark coupling in murine arterial smooth muscle cells. *Am J Physiol Heart Circ Physiol* **290**, H2309–H2319.

Cheng H, Lederer WJ & Cannell MB (1993). Calcium sparks: elementary events underlying excitation-contraction coupling in heart muscle. *Science* **262**, 740–744.

Ching LL, Williams AJ & Sitsapesan R (2000). Evidence for Ca^{2+} activation and inactivation sites on the luminal side of the cardiac ryanodine receptor complex. *Circ Res* **87**, 201–206.

Clapham DE, Runnels LW & Strubing C (2001). The TRP ion channel family. *Nat Rev Neurosci* **2**, 387–396.

Cleemann L, Wang W & Morad M (1998). Two-dimensional confocal images of organization, density, and gating of focal Ca^{2+} release sites in rat cardiac myocytes. *Proc Natl Acad Sci U S A* **95**, 10984–10989.

Collier ML, Ji G, Wang Y & Kotlikoff MI (2000). Calcium-induced calcium release in smooth muscle: loose coupling between the action potential and calcium release. *J Gen Physiol* **115**, 653–662.

Collier ML, Thomas AP & Berlin JR (1999). Relationship between L-type Ca^{2+} current and unitary sarcoplasmic reticulum Ca^{2+} release events in rat ventricular myocytes. *J Physiol* **516**, 117–128.

Fabiato A & Fabiato F (1979). Calculator programs for computing the composition of the solutions containing multiple metals and ligands used for experiments in skinned muscle cells. *J Physiol (Paris)* **75**, 463–505.

Furstenau M, Lohn M, Ried C, Luft FC, Haller H & Gollasch M (2000). Calcium sparks in human coronary artery smooth muscle cells resolved by confocal imaging. *J Hypertens* **18**, 1215–1222.

Gollasch M, Haller H, Schultz G & Hescheler J (1991). Thyrotropin-releasing hormone induces opposite effects on Ca^{2+} channel currents in pituitary cells by two pathways. *Proc Natl Acad Sci U S A* **88**, 10262–10266.

Gollasch M, Ried C, Bychkov R, Luft FC & Haller H (1996). K^+ currents in human coronary artery vascular smooth muscle cells. *Circ Res* **78**, 676–688.

Gollasch M, Wellman GC, Knot HJ, Jaggar JH, Damon DH, Bonev AD & Nelson MT (1998). Ontogeny of local sarcoplasmic reticulum Ca^{2+} signals in cerebral arteries: Ca^{2+} sparks as elementary physiological events. *Circ Res* **83**, 1104–1114.

Gordienko DV & Bolton TB (2002). Crosstalk between ryanodine receptors and IP_3 receptors as a factor shaping spontaneous Ca^{2+}-release events in rabbit portal vein myocytes. *J Physiol* **542**, 743–762.

Grabner M, Dirksen RT, Suda N & Beam KG (1999). The II–III loop of the skeletal muscle dihydropyridine receptor is responsible for the bi-directional coupling with the ryanodine receptor. *J Biol Chem* **274**, 21913–21919.

Herrera GM, Heppner TJ & Nelson MT (2001). Voltage dependence of the coupling of Ca^{2+} sparks to BK_{Ca} channels in urinary bladder smooth muscle. *Am J Physiol Cell Physiol* **280**, C481–C490.

Hofmann F, Lacinova L & Klugbauer N (1999). Voltage-dependent calcium channels: from structure to function. *Rev Physiol Biochem Pharmacol* **139**, 33–87.

Imaizumi Y, Torii Y, Ohi Y, Nagano N, Atsuki K, Yamamura H, Muraki K, Watanabe M & Bolton TB (1998). Ca^{2+} images and K^+ current during depolarization in smooth muscle cells of the guinea-pig vas deferens and urinary bladder. *J Physiol* **510**, 705–719.

Iwasaki H, Mori Y, Hara Y, Uchida K, Zhou H & Mikoshiba K (2001). 2-Aminoethoxydiphenyl borate (2-APB) inhibits capacitative calcium entry independently of the function of inositol 1,4,5-trisphosphate receptors. *Receptors Channels* **7**, 429–439.

Jaggar JH, Porter VA, Lederer WJ & Nelson MT (2000). Calcium sparks in smooth muscle. *Am J Physiol Cell Physiol* **278**, C235–C256.

Jaggar JH, Stevenson AS & Nelson MT (1998). Voltage dependence of Ca^{2+} sparks in intact cerebral arteries. *Am J Physiol Cell Physiol* **274**, C1755–C1761.

Kamishima T, Davies NW & Standen NB (2000). Mechanisms that regulate $[Ca^{2+}]_i$ following depolarization in rat systemic arterial smooth muscle cells. *J Physiol* **522**, 285–295.

Kamishima T & McCarron JG (1996). Depolarization-evoked increases in cytosolic calcium concentration in isolated smooth muscle cells of rat portal vein. *J Physiol* **492**, 61–74.

Klein MG, Lacampagne A & Schneider MF (1997). Voltage dependence of the pattern and frequency of discrete Ca^{2+} release events after brief repriming in frog skeletal muscle. *Proc Natl Acad Sci U S A* **94**, 11061–11066.

Knot HJ, Standen NB & Nelson MT (1998). Ryanodine receptors regulate arterial diameter and wall $[Ca^{2+}]$ in cerebral arteries of rat via Ca^{2+}-dependent K^+ channels. *J Physiol* **508**, 211–221.

Kotlikoff MI (2003). Calcium-induced calcium release in smooth muscle: the case for loose coupling. *Prog Biophys Mol Biol* **83**, 171–191.

Kuhbandner S, Brummer S, Metzger D, Chambon P, Hofmann F & Feil R (2000). Temporally controlled somatic mutagenesis in smooth muscle. *Genesis* **28**, 15–22.

Lohn M, Furstenau M, Sagach V, Elger M, Schulze W, Luft FC, Haller H & Gollasch M (2000). Ignition of calcium sparks in arterial and cardiac muscle through caveolae. *Circ Res* **87**, 1034–1039.

Lohn M, Jessner W, Furstenau M, Wellner M, Sorrentino V, Haller H, Luft FC & Gollasch M (2001*a*). Regulation of calcium sparks and spontaneous transient outward currents by RyR3 in arterial vascular smooth muscle cells. *Circ Res* **89**, 1051–1057.

Lohn M, Lauterbach B, Haller H, Pongs O, Luft FC & Gollasch M (2001*b*). β_1-Subunit of BK channels regulates arterial wall [Ca^{2+}] and diameter in mouse cerebral arteries. *J Appl Physiol* **91**, 1350–1354.

Lohn M, Muzzulini U, Essin K, Tsang SY, Kirsch T, Litteral J, Waldron P, Conrad H, Klugbauer N, Hofmann F, Haller H, Luft FC, Huang Y & Gollasch M (2002). Cilnidipine is a novel slow-acting blocker of vascular L-type calcium channels that does not target protein kinase C. *J Hypertens* **20**, 885–893.

Lopez-Lopez JR, Shacklock PS, Balke CW & Wier WG (1995). Local calcium transients triggered by single L-type calcium channel currents in cardiac cells. *Science* **268**, 1042–1045.

Marks TN & Jones SW (1992). Calcium currents in the A7r5 smooth muscle-derived cell line. An allosteric model for calcium channel activation and dihydropyridine agonist action. *J Gen Physiol* **99**, 367–390.

McCarthy RT & Cohen CJ (1989). Nimodipine block of calcium channels in rat vascular smooth muscle cell lines. Exceptionally high-affinity binding in A7r5 and A10 cells. *J Gen Physiol* **94**, 669–692.

Moosmang S, Schulla V, Welling A, Feil R, Feil S, Wegener JW, Hofmann F & Klugbauer N (2003). Dominant role of smooth muscle L-type calcium channel Cav1.2 for blood pressure regulation. *EMBO J* **22**, 6027–6034.

Navedo MF, Amberg GC, Nieves M, Molkentin JD & Santana LF (2006). Mechanisms underlying heterogeneous Ca^{2+} sparklet activity in arterial smooth muscle. *J Gen Physiol* **127**, 611–622.

Navedo MF, Amberg GC, Votaw VS & Santana LF (2005). Constitutively active L-type Ca^{2+} channels. *Proc Natl Acad Sci U S A* **102**, 11112–11117.

Nelson MT, Cheng H, Rubart M, Santana LF, Bonev AD, Knot HJ & Lederer WJ (1995). Relaxation of arterial smooth muscle by calcium sparks. *Science* **270**, 633–637.

Nelson MT, Patlak JB, Worley JF & Standen NB (1990). Calcium channels, potassium channels, and voltage dependence of arterial smooth muscle tone. *Am J Physiol Cell Physiol* **259**, C3–C18.

Owsianik G, Talavera K, Voets T & Nilius B (2006). Permeation and selectivity of TRP channels. *Annu Rev Physiol* **68**, 685–717.

Papadopoulos S, Leuranguer V, Bannister RA & Beam KG (2004). Mapping sites of potential proximity between the dihydropyridine receptor and RyR1 in muscle using a cyan fluorescent protein-yellow fluorescent protein tandem as a fluorescence resonance energy transfer probe. *J Biol Chem* **279**, 44046–44056.

Peppiatt CM, Collins TJ, Mackenzie L, Conway SJ, Holmes AB, Bootman MD, Berridge MJ, Seo JT & Roderick HL (2003). 2-Aminoethoxydiphenyl borate (2-APB) antagonises inositol 1,4,5-trisphosphate-induced calcium release, inhibits calcium pumps and has a use-dependent and slowly reversible action on store-operated calcium entry channels. *Cell Calcium* **34**, 97–108.

Perez GJ, Bonev AD & Nelson MT (2001). Micromolar Ca^{2+} from sparks activates Ca^{2+}-sensitive K^+ channels in rat cerebral artery smooth muscle. *Am J Physiol Cell Physiol* **281**, C1769–C1775.

Perez GJ, Bonev AD, Patlak JB & Nelson MT (1999). Functional coupling of ryanodine receptors to KCa channels in smooth muscle cells from rat cerebral arteries. *J Gen Physiol* **113**, 229–238.

Pluger S, Faulhaber J, Furstenau M, Lohn M, Waldschutz R, Gollasch M, Haller H, Luft FC, Ehmke H & Pongs O (2000). Mice with disrupted BK channel $\beta 1$ subunit gene feature abnormal Ca^{2+} spark/STOC coupling and elevated blood pressure. *Circ Res* **87**, E53–E60.

Remillard CV, Zhang WM, Shimoda LA & Sham JS (2002). Physiological properties and functions of Ca^{2+} sparks in rat intrapulmonary arterial smooth muscle cells. *Am J Physiol Lung Cell Mol Physiol* **283**, L433–L444.

Rueda A & Valdivia HH (2006). Sorcin reduces the amplitude, duration and spatial spread of Ca^{2+} sparks in permeabilized vascular myocytes. *Biophys J* **90**, 1090-Pos (abstract).

Ruth P, Flockerzi V, Von Nettelbladt E, Oeken J & Hofmann F (1985). Characterization of the binding sites for nimodipine and (–)-desmethoxyverapamil in bovine cardiac sarcolemma. *Eur J Biochem* **150**, 313–322.

Sausbier M, Arntz C, Bucurenciu I, Zhao H, Zhou XB, Sausbier U, Feil S, Kamm S, Essin K, Sailer CA, Abdullah U, Krippeit-Drews P, Feil R, Hofmann F, Knaus HG, Kenyon C, Shipston MJ, Storm JF, Neuhuber W, Korth M, Schubert R, Gollasch M & Ruth P (2005). Elevated blood pressure linked to primary hyperaldosteronism and impaired vasodilation in BK channel-deficient mice. *Circulation* **112**, 60–68.

Shen JX, Wang S, Song LS, Han T & Cheng H (2004). Polymorphism of Ca^{2+} sparks evoked from in-focus Ca^{2+} release units in cardiac myocytes. *Biophys J* **86**, 182–190.

Slesinger PA & Lansman JB (1996). Reopening of single L-type Ca^{2+} channels in mouse cerebellar granule cells: dependence on voltage and ion concentration. *J Physiol* **491**, 335–345.

Stern MD (1992). Buffering of calcium in the vicinity of a channel pore. *Cell Calcium* **13**, 183–192.

Tsugorka A, Rios E & Blatter LA (1995). Imaging elementary events of calcium release in skeletal muscle cells. *Science* **269**, 1723–1726.

van Rossum DB, Patterson RL, Ma HT & Gill DL (2000). Ca^{2+} entry mediated by store depletion, S-nitrosylation, and TRP3 channels. Comparison of coupling and function. *J Biol Chem* **275**, 28562–28568.

Wang SQ, Song LS, Lakatta EG & Cheng H (2001). Ca^{2+} signalling between single L-type Ca^{2+} channels and ryanodine receptors in heart cells. *Nature* **410**, 592–596.

Wang SQ, Wei C, Zhao G, Brochet DX, Shen J, Song LS, Wang W, Yang D & Cheng H (2004). Imaging microdomain Ca^{2+} in muscle cells. *Circ Res* **94**, 1011–1022.

Wellman GC, Santana LF, Bonev AD & Nelson MT (2001). Role of phospholamban in the modulation of arterial Ca^{2+} sparks and Ca^{2+}-activated K^+ channels by cAMP. *Am J Physiol Cell Physiol* **281**, C1029–C1037.

White C & McGeown JG (2003). Inositol 1,4,5-trisphosphate receptors modulate Ca^{2+} sparks and Ca^{2+} store content in vas deferens myocytes. *Am J Physiol Cell Physiol* **285**, C195–C204.

ZhuGe R, Tuft RA, Fogarty KE, Bellve K, Fay FS & Walsh JV Jr (1999). The influence of sarcoplasmic reticulum Ca^{2+} concentration on Ca^{2+} sparks and spontaneous transient outward currents in single smooth muscle cells. *J Gen Physiol* **113**, 215–228.

Zima AV & Blatter LA (2004). Inositol-1,4,5-trisphosphate-dependent Ca^{2+} signalling in cat atrial excitation–contraction coupling and arrhythmias. *J Physiol* **555**, 607–615.

Acknowledgements

We are indebted to Susanne Paparisto for her excellent technical assistance. The Deutsche Forschungsgemeinschaft supported this work.

Supplemental material

Online supplemental material for this paper can be accessed at:
http://jp.physoc.org/cgi/content/full/jphysiol.2007.138982/DC1
and
http://www.blackwell-synergy.com/doi/suppl/10.1113/jphysiol.2007.138982